EUROPEAN ORGANIZATION FOR NUCLEAR RESEARCH

ALEPH 2002-024 CONF 2002-013
DELPHI 2002-088-CONF-621
L3 Note 2766
OPAL Technical Note TN721
LHWG Note/2002-01
July 19, 2002

Search for the Standard Model Higgs Boson at LEP

ALEPH, DELPHI, L3 and OPAL Collaborations

The LEP Working Group for Higgs Boson Searches

Abstract

The four LEP collaborations, ALEPH, DELPHI, L3 and OPAL, have collected 2461 pb^{-1} of e^+e^- collision data at centre-of-mass energies between 189 and 209 GeV, of which 536 pb^{-1} have energies above 206 GeV. The data have been used to search for the Standard Model Higgs boson. The search results of the four collaborations are combined and examined for their consistency with two hypotheses: (a) the Standard Model background hypothesis and (b) the signal plus background hypothesis. The confidence levels for the two hypotheses have been computed in a likelihood analysis as a function of the hypothetical Higgs boson mass. The evolution of the likelihood as a function of the test-mass shows a slight preference for the signal plus background hypothesis for a Higgs boson mass in the vicinity of 116 GeV, where the confidence level for the signal plus background hypothesis is 37% while that for the background hypothesis is about 8%. A lower bound of 114.4 GeV has been established, at the 95% confidence level, for the mass of the Standard Model Higgs boson.

The results presented in this note are preliminary

Contributed paper for ICHEP'02 (Amsterdam, July 2002)

1 Introduction

The Higgs mechanism [1] plays a central role in the unification of the electromagnetic and weak interactions by providing mass to the intermediate vector bosons W and Z, without violating local gauge invariance. Within the Standard Model [2], the Higgs mechanism predicts a single neutral scalar particle, the Higgs boson. Its mass is not predicted by the theory, but the self-consistency of the Standard Model up to an arbitrary scale Λ imposes an upper [3] and a lower bound [4] on the mass, which depend on Λ. For example, at Λ close to the grand unification scale, $\Lambda_{GUT} \approx 10^{16}$ GeV, the mass is confined between about 130 and 190 GeV [5]; such values are only slightly beyond the range of sensitivity of LEP. The discovery of a Higgs boson with mass less than 130 GeV would be an important indication for new physics to set in at energies below the GUT scale.

Indirect experimental constraints are obtained from the precision measurements of the electroweak parameters, which depend logarithmically on the Higgs boson mass through radiative corrections. Currently these measurements constrain the Standard Model Higgs boson mass to $m_{\mathrm{H}} = 81^{+52}_{-33}$ GeV or to values smaller than 193 GeV, at the 95% confidence level [6].

The data collected by the four LEP collaborations prior to the year 2000 have not revealed any indication for the Standard Model Higgs boson [7]. In the year 2000, substantial data samples were collected at centre-of-mass energies exceeding 206 GeV. In these data, ALEPH [8] observed an excess of events consistent with the production of a Standard Model Higgs boson with mass in the vicinity of 115 GeV. L3 [9] and OPAL [10] also reported slight excesses in this region, while DELPHI [11] reported a slight deficit with respect to the background expectation. The LEP Higgs Working Group (LHWG) has combined the preliminary results from ALEPH, DELPHI and OPAL with the final results of L3 [12], which became available in June 2001, and submitted a preliminary combined result [13] to the EPS-HEP'01 conference in Budapest and the LP'01 conference in Rome.

Following the previous combination, ALEPH, DELPHI and OPAL have produced final results in which definitive calibrations of the detectors and centre-of-mass energies have been included and which follow, in some cases, a revision of the data analysis procedures. The final ALEPH result is published in Ref. [14] while the final DELPHI [15] and OPAL [16] results have recently been submitted for publication. In Table 1, the final results are compared to those which were used in the preliminary LHWG combination; the confidence levels for the background hypothesis, $1 - \mathrm{CL_b}$ (see Section 2 below), and the 95% confidence level lower bounds for the Higgs boson mass are listed.

In this paper we present the results from a combination which is based on the final publications [12, 14, 15, 16]. The data span the range of centre-of-mass energies from 189 GeV to 209 GeV. The integrated luminosities of the data samples are given in Table 2 for the full range of energies and for the subset with energies larger than 206 GeV.

We also present an upper bound on the HZZ coupling in non-standard models which assume, however, that the Higgs boson decay properties are those of the Standard Model. In order to

		ALEPH	DELPHI	L3	OPAL
$1-\mathrm{CL_b}$	Preliminary	1.5×10^{-3} [8]	0.77 [11]	0.32 [12]	0.20 [10]
	Final	2.4×10^{-3} [14]	0.73 [15]	0.32 [12]	0.50 [16]
Mass bound [GeV]	Preliminary	111.1 [8]	114.3 [11]	112.0 [12]	109.7 [10]
	Final	111.5 [14]	114.1 [15]	112.0 [12]	112.7 [16]

Table 1: Comparison of the final results of the individual experiments and those which were available at the time of the preliminary LHWG combination (summer 2001). Upper part: confidence levels, $1-\mathrm{CL_b}$, for the background hypothesis. The ALEPH values are quoted at the test-masses (close to 115 GeV) which minimize this probability; for the other three experiments the values are quoted at 115 GeV. Lower part: 95% confidence level lower bounds for the mass of the Standard Model Higgs boson.

	ALEPH	DELPHI	L3	OPAL	LEP
$E_{cm} \geq 189$ GeV	629	608	627	596	2461 pb^{-1}
$E_{cm} \geq 206$ GeV	130	138	139	129	536 pb^{-1}

Table 2: Integrated luminosities (pb^{-1}) of the data samples of the four experiments and their sum (LEP). Subsets taken at energies larger than 206 GeV are listed separately.

cover the low-mass domain, the LEP1 data collected at the Z resonance have been combined with the high-energy LEP2 data.

2 Analysis and Combination Procedure

At LEP energies, the Standard Model Higgs boson is expected to be produced mainly in association with a Z boson through the Higgsstrahlung process, $\mathrm{e^+e^-}\rightarrow\mathrm{HZ}$ [17]. Small additional contributions are expected from t-channel W and Z boson fusion processes, which produce a Higgs boson and a pair of neutrinos or electrons, respectively, in the final state [18]. For masses lower than 120 GeV, which are relevant for searches at LEP, the Standard Model Higgs boson is expected to decay mainly into $\mathrm{b\bar{b}}$ quark pairs (74% for a mass of 115 GeV) while other decays, to $\tau^+\tau^-$, $\mathrm{WW^*}$, gg ($\approx$ 7% each), and to $\mathrm{c\bar{c}}$ ($\approx$ 4%) make up for the rest of the decay width. The final-state topologies are determined by these decay properties of the Higgs boson and by those of the associated Z boson. The searches at LEP encompass the four-jet final state $(\mathrm{H}\rightarrow\mathrm{b\bar{b}})(\mathrm{Z}\rightarrow\mathrm{q\bar{q}})$, the missing energy final state $(\mathrm{H}\rightarrow\mathrm{b\bar{b}})(\mathrm{Z}\rightarrow\nu\bar{\nu})$, the leptonic final state $(\mathrm{H}\rightarrow\mathrm{b\bar{b}})(\mathrm{Z}\rightarrow\ell^+\ell^-)$ where ℓ denotes an electron or a muon, and the tau lepton final states $(\mathrm{H}\rightarrow\mathrm{b\bar{b}})(\mathrm{Z}\rightarrow\tau^+\tau^-)$ and $(\mathrm{H}\rightarrow\tau^+\tau^-)(\mathrm{Z}\rightarrow\mathrm{q\bar{q}})$.

A preselection is applied by each experiment to reduce the main background, from two-

photon processes and from radiative returns to the Z boson, $e^+e^- \to Z\gamma(\gamma)$. The remaining background, mainly from fermion pairs , WW, and ZZ, (possibly with photon or gluon radiation), is further reduced by analyses which combine likelihood and neural network techniques and make use of the expected differences between the signal and the background processes. The requirement of b-flavour, abundant in the decay of the Higgs boson, plays an important role in the discrimination between signal and background, as does the reconstructed Higgs boson candidate mass, $m_{\rm H}^{rec}$. The detailed implementation of these analyses is different for each experiment [12, 14, 15, 16].

2.1 Input from the Experiments

The input from the LEP experiments which is used in the combination is provided channel by channel. The word "channel" designates any subset of the data where a Higgs boson search has been carried out. These subsets may correspond to different final-state topologies, to data sets collected at different centre-of-mass energies or to the subsets of data obtained by different experiments. In most channels, the input is binned in two variables: the reconstructed Higgs boson mass $m_{\rm H}^{rec}$, and a variable $\mathcal{G}$ which combines many event features allowing discrimination on a statistical basis between the Higgs boson signal and the background processes.

In a given bin i of the plane defined by $m_{\rm H}^{rec}$ and $\mathcal{G}$, the experiments provide the number n_i of selected data events, the expected background rate b_i, and the expected signal $s_i(m_{\rm H})$ for a set of hypothetical Higgs boson masses (test-mass $m_{\rm H}$ hereafter). In those channels where the event selection also depends explicitly on the test-mass, the values of n_i and b_i are given for a set of $m_{\rm H}$ values, just like s_i. For a given test-mass, a weight of s/b can thus be assigned to each selected candidate, depending on the bin of ($m_{\rm H}^{rec}$, $\mathcal{G}$) where it is reconstructed. The estimation of s_i and b_i makes use of detailed Monte Carlo simulations which take into account all known experimental features such as the centre-of-mass energy and integrated luminosity of the data samples, cross-sections and decay branching ratios for the signal and background processes, selection efficiencies, experimental resolutions with non-Gaussian contributions and systematic errors with their correlations. Since the simulation is done at fixed sets of centre-of-mass energies and test-masses, interpolations are applied (see e.g., Ref. [19]) to obtain the rates and distributions for arbitrary energies and test-masses. In order to avoid problems which might arise in some bins due to low Monte Carlo statistics, smoothing procedures are applied (see e.g., Ref. [20]) which combine the available information with the information in the neighbouring bins.

3 Hypothesis Testing

The observed data configuration in the ($m_{\rm H}^{rec}$, $\mathcal{G}$) plane is subjected to a likelihood test of two hypothetical scenarios. In the background scenario it is assumed that the data receive contributions from the Standard Model background processes only while in the signal+background

scenario the contributions from a Higgs boson of test-mass $m_{\rm H}$ are assumed in addition. The expressions for the corresponding likelihoods, $\mathcal{L}_b$ and $\mathcal{L}_{s+b}$, are given in Appendix A. The ratio

$$Q = \mathcal{L}_{s+b}/\mathcal{L}_b \tag{1}$$

serves as test-statistic which allows any data configuration, observed or simulated, to be ranked between the background and signal+background hypotheses. This choice of test-statistic makes the most efficient use of the information contained in the event configuration selected in a search experiment, similarly to the principle of maximum likelihood which gives the most efficient estimators of parameters in a measurement. For convenience, the logarithmic form of Q

$$-2\ln Q = 2s_{tot} - 2\sum_i n_i \ln[1 + s_i/b_i] \tag{2}$$

is used since, in the limit of high statistics, $-2\ln Q$ corresponds to the difference in χ^2 of the two hypotheses. Also, this expression is linear in the weights $\ln(1 + s/b)$ of individual candidates. In this expression, $s_{tot} = \sum_i s_i$ is the total expected signal rate. For a more complete form of the test-statistic, incorporating discriminant variable information, see Appendix A.

Figure 1 shows the test-statistic $-2\ln Q$ as a function of the test-mass for the present combination. The expected curves and the 68% and 95% probability bands (shown here only for the background hypothesis) are obtained by replacing the observed data configuration by a large number of simulated event configurations for the background and signal plus background hypotheses. There is a broad minimum in the observed $-2\ln Q$ which extends from $m_{\rm H} \approx$ 115 GeV to about 118 GeV. The expectation for signal plus background crosses the observation at about 116 GeV, indicating that a Standard Model Higgs boson with mass in this range is the favoured interpretation.

The observed curve in Figure 1 is in excess of the background expectation over a wide range of masses. This can be explained by non-Gaussian contributions to the experimental resolution; however, a similar behaviour would be expected from statistical fluctuations of the background.

In Figures 2 and 3, the likelihood test is applied to subsets of the data, from individual experiments and final-state topologies. One can see that the signal-like behaviour mainly originates from the ALEPH data and that it is concentrated in the four-jet final state. These figures illustrate the rapid decrease of discriminating power, indicated by the distance between the expected curves, as the test-mass approaches the kinematic limit of the HZ signal process. One should be aware that no individual LEP experiment has the statistical power to distinguish between the background and the signal+background hypotheses for a test-mass larger than about 115 GeV at the level of two standard deviations (see the intersections of the signal+background curve with the lower edge of the light/yellow shaded bands); as for the individual final-state topologies, only the LEP combined four-jet channel is sufficiently powerful to make the distinction. The comparison of Figures 1 and 2 illustrates, on the other hand, the gain in sensitivity when the data of the four experiments are added.

3.1 Contributions from Single Candidates

The test-statistic $-2\ln Q$ is built up from individual event weights $\ln(1+s/b)$. The candidates which have the highest weight at $m_{\rm H} = 115$ GeV are listed in Table 3. For these events, the

	Expt	E_{cm}	Decay channel	$m_{\rm H}^{rec}$ (GeV)	$\ln(1+s/b)$ at 115 GeV
1	ALEPH	206.6	4-jet	114.1	1.76
2	ALEPH	206.6	4-jet	114.4	1.44
3	ALEPH	206.4	4-jet	109.9	0.59
4	L3	206.4	E-miss	115.0	0.53
5	ALEPH	205.1	Lept	117.3	0.49
6	ALEPH	206.5	Taus	115.2	0.45
7	OPAL	206.4	4-jet	108.2	0.43
8	ALEPH	206.4	4-jet	114.4	0.41
9	L3	206.4	4-jet	108.3	0.30
10	DELPHI	206.6	4-jet	110.7	0.28
11	ALEPH	207.4	4-jet	102.8	0.27
12	DELPHI	206.6	4-jet	97.4	0.23
13	OPAL	201.5	E-miss	111.2	0.22
14	L3	206.4	E-miss	110.1	0.21
15	ALEPH	206.5	4-jet	114.2	0.19
16	DELPHI	206.6	4-jet	108.2	0.19
17	L3	206.6	4-jet	109.6	0.18

Table 3: Properties of the candidates contributing to $-2\ln Q$ with the highest weight at $m_{\rm H} = 115$ GeV. The applied selection, $\ln(1+s/b) > 0.18$ (i.e. $s/b > 0.2$) at $m_{\rm H} = 115$ GeV, retains 17 candidates while the expected signal and background rates are 8.42 and 15.9 events, respectively. The experiment of origin, the centre-of-mass energy, the decay channel, the reconstructed mass and the weight at $m_{\rm H} = 115$ are listed.

evolution of $\ln(1+s/b)$ with test-mass is shown in Figure 4. Typically, the weight is largest for $m_{\rm H} \approx m_{\rm H}^{rec}$ but there is a sizeable weight over an extended domain of test-masses due to the experimental resolution.

The distributions of event weights, for the test-mass fixed at $m_{\rm H}$ =110, 115 and 116 GeV, are shown in the upper, middle and lower parts of Figure 5 ($\log_{10} s/b$ is plotted for better visibility). The plots to the right show the integrals of these distributions starting from the high end of $\log_{10} s/b$ (the bins are thus correlated). In the plots for $m_{\rm H} = 110$ GeV, the data show clear preference for the background hypothesis over the signal+background hypothesis. In the plots for $m_{\rm H}$ =115 and 116 GeV, there may be a slight preference for the signal+background hypothesis, but the separation of the expected curves is rather limited.

The expected signal rates for three test-masses, the expected background rates, and the

observed event rates, are listed in Table 4 for various cuts in the event weight.

$m_{\rm H}$	$\ln(1+s/b)_{min}$	Expected signal	Expected backgd.	Data
110 GeV	0.01	78.7	490.8	496
	0.1	63.9	135.6	155
	0.18	55.6	78.6	89
	0.5	36.3	22.0	18
	1	20.7	6.54	7
	2	2.74	0.30	1
115 GeV	0.01	17.86	262.0	281
	0.1	10.85	33.1	37
	0.18	8.42	15.8	17
	0.5	4.26	3.27	5
	1	1.57	0.54	2
	2	0.17	0.02	0
116 GeV	0.01	11.15	218.2	242
	0.1	5.62	20.1	21
	0.18	4.04	8.93	9
	0.5	1.52	1.31	3
	1	0.45	0.17	1
	2	0.02	0.002	0

Table 4: Expected signal and background rates, and the observed event rates, for test-masses of 110, 115, and 116 GeV, for various cuts in the event weight $\ln(1+s/b)$.

3.2 The Reconstructed Higgs Boson Mass

The reconstructed Higgs boson mass $m_{\rm H}^{rec}$ is one of several variables which contribute to the discrimination between the signal and the background, and thus to the likelihood ratio Q. Figure 6 shows the distributions for this important discriminating variable at various levels of signal purity. Note that these distributions do not enter directly into the calculation of confidence levels and are produced here only for illustration. Indeed, in some of the channels which enter the combination, the event selection and weight calculation depends explicitly on the test-mass, and the resulting distribution of $m_{\rm H}^{rec}$ would thus be biased. The distributions in Figure 6 are, therefore, obtained with special selection cuts in variables which are only mildly correlated with $m_{\rm H}^{rec}$ (e.g. b-tag variables).

4 Confidence Levels

The expected distributions of the test-statistic $-2\ln Q$, resulting from the present LEP-combined analysis, are shown in Figure 7 (upper part) for a test-mass of 116 GeV (a "slice" of Figure 1, at $m_{\rm H} = 116$ GeV). These distributions for the background and the signal+background hypotheses are probability density functions (pdf), which include both the effects of random statistical variations in the numbers of events and also systematic uncertainties affecting the expected rates.

The vertical line indicates the observed value of $-2\ln Q$; it is found to lie within the distribution for the signal+background hypothesis and in the tail of the distribution for the background hypothesis. The integral of the pdf for signal+background from $+\infty$ to the observed value, $\mathrm{CL_{s+b}}$, expresses the compatibility of the observation with the signal+background hypothesis. Similarly, the integral of the pdf for background from $-\infty$ to the observed value, $1-\mathrm{CL_b}$, quantifies the compatibility with the background hypothesis: given a large number of measurements and no signal, it is the probability to obtain an event configuration more signal-like than the one observed.

The distributions of $-2\ln Q$ for test-masses $m_{\rm H} = 110$ and 120 GeV, in the lower part of Figure 7, demonstrate the significant discriminating power of the LEP-combined data for lower $m_{\rm H}$ and its rapid decrease at the end of the kinematic range of the HZ signal process.

The values of $1-\mathrm{CL_b}$ and $\mathrm{CL_{s+b}}$, obtained for $m_{\rm H} = 116$ GeV, are listed in Table 5 for all LEP data combined and for various sub-samples.

	$1-\mathrm{CL_b}$	$\mathrm{CL_{s+b}}$
LEP	0.099	0.369
ALEPH	2.41×10^{-3}	0.956
DELPHI	0.874	0.033
L3	0.348	0.408
OPAL	0.543	0.208
Four-jet	5.70×10^{-2}	0.676
All but four-jet	0.368	0.217

Table 5: The background confidence level $1-\mathrm{CL_b}$ and the signal+background confidence level $\mathrm{CL_{s+b}}$ at $m_{\rm H} = 116$ GeV, for all LEP data combined and for various subsets of the data. The numbers for the four-jet and all-but-four-jet final states are obtained with the data of the four experiments combined.

Figure 8 shows $1-\mathrm{CL_b}$ for test-masses in the range from 100 to 120 GeV. The value of about 8×10^{-2} observed in the vicinity of 116 GeV translates into 1.7 standard deviations from the background hypothesis (see Appendix B for the conversion). The structure in the vicinity of 100 GeV was reported in the LEP combination of 1999 [21] using data up to 189 GeV energy;

its significance has not noticably increased with the addition of new data. Also, the deviation from the background expectation is much smaller than what is expected from a Higgs boson with mass of about 100 GeV.

It should be remembered that the confidence level $1-\mathrm{CL_b}$ refers to *local* fluctuations of the background. To obtain the probability for such a fluctuation to appear anywhere within a given mass range of interest, a multiplicative factor has to be applied which is approximately equal to the width of the mass range of interest divided by the mass resolution. In the present case, the range of interest is limited from below by previous exclusion limits (107.9 GeV [7]) and from above by the kinematic limit of the HZ signal process (about 117 GeV). Since the mass resolution averaged over the final-state topologies and the four experiments is about 3.5 GeV, this multiplicative factor is about 2.5.

Figure 9 shows $1-\mathrm{CL_b}$ as a function of the test-mass for subsets of the data, from individual experiments, the four-jet decay channel, and all decay channels but the four-jet combined. In the latter two cases the contributions from the four experiments are added.

5 Bounds for the Higgs Boson Mass and Coupling

The ratio $\mathrm{CL_s} = \mathrm{CL_{s+b}}/\mathrm{CL_b}$ as a function of the test-mass, shown in Figure 10, is used to derive a lower bound for the Standard Model Higgs boson mass; the test-mass giving $\mathrm{CL_s} = 0.05$ defines the lower bound at the 95% confidence level (see Appendix A). The expected and

	Expected limit (GeV)	Observed limit (GeV)
LEP	115.3	114.4
ALEPH	113.5	111.5
DELPHI	113.3	114.3
L3	112.4	112.0
OPAL	112.7	112.8
Four-jet channel	114.5	113.3
All but four-jet	114.2	114.2

Table 6: Expected (median) and observed 95% confidence level lower bounds on the Standard Model Higgs boson mass, for all LEP data combined and for various subsets of the data. The numbers for the four-jet and all but four-jet final states are obtained with the data of the four experiments combined.

observed lower bounds are listed in Table 6. The 95% confidence level lower bound for the mass of the Standard Model Higgs boson is thus 114.4 GeV.

The LEP data are used also to set a 95% confidence level upper bound on the HZZ coupling in non-standard models which assume universal scaling of the Higgs couplings to the Z and W bosons, and for which the Higgs boson decay properties are those of the Standard Model.

Figure 11 shows the upper bound on $\xi^2 = (g_{HZZ}/g^{SM}_{HZZ})^2$, the square of the ratio of the coupling in such models to the Standard Model coupling, as a function of the Higgs boson mass. In deriving this limit, the LEP1 data collected at the Z resonance have been combined with the high-energy LEP2 data.

6 Summary of the Results

Combining the data from the four LEP experiments, a lower bound is set on the mass of the Standard Model Higgs boson, which is 114.4 GeV at the 95% confidence level. An excess is observed which could be interpreted as production of a Standard Model Higgs boson with a mass higher than this limit. The excess is concentrated mainly in the data sets with centre-of-mass energies higher than 206 GeV. The likelihood test designates the range from 115 to 118 for the preferred mass, where the confidence level for the signal plus background hypothesis is 37% while that for the background hypothesis is about 8%. This deviation from the Standard Model background hypothesis is mainly driven by the ALEPH data and is concentrated in the four-jet final state.

The LEP1 and LEP2 data have been used in conjunction to set an upper bound on the HZZ coupling for Higgs boson masses between 12 and 115 GeV mass; these bounds are valid in non-standard models which assume a universal scaling of the Higgs couplings to the vector bosons Z and W and where the Higgs decay properties are assumed to be those predicted by the Standard Model.

ACKNOWLEDGEMENTS

We congratulate our colleagues from the LEP Accelerator Division for the successful running in the year 2000 at the highest energies, and would like to express our thanks to the engineers and technicians in all our institutions for their contributions to the excellent performance of the four LEP experiments. The LEP Higgs Working Group acknowledges the fruitful cooperation between the experiments in developing the combination procedures and applying them to the LEP data.

Appendix A:

Combined Confidence Levels

In the Standard Model, the signal and background rates are predicted channel by channel; the corresponding search results can thus be combined for a better overall sensitivity. Furthermore, data sets from different LEP energies and different experiments can also be added together.

The combined LEP data are submitted to a test with two hypotheses: the background ("b") hypothesis, which assumes no Higgs boson to be present in the mass range investigated, and the signal+background ("s+b") hypothesis, where Higgs bosons are assumed to be produced according to the Standard Model, its production cross section and the branching fractions being fixed by the hypothetical Higgs boson mass (test-mass m_{H}). A global test-statistic Q is constructed which allows the experimental result, $Q_{observed}$, to be ranked between the b-like and s+b-like situations. It utilises the number of selected events and various distributions which provide discrimination between signal and background (e.g., the reconstructed mass or b-tag variables). The test-statistic takes into account all known experimental details such as detection efficiencies, signal-to-background ratios and resolution functions with non-Gaussian tails, systematic errors with their correlations, and provides a single value for a given model hypothesis, m_{H}.

To determine the probability distribution for Q which, for searches with small numbers of signal events, tends to be non-Gaussian, a large number of Monte Carlo experiments are generated for the background hypothesis and separately for a set of signal+background models with fixed values of m_{H}. The resulting distributions of $Q(m_{\mathrm{H}})$ are normalised to become probability density functions, and integrated to form the confidence levels $1-\mathrm{CL_b}(m_{\mathrm{H}})$ and $\mathrm{CL_{s+b}}(m_{\mathrm{H}})$; these express the probabilities that the outcome of an experiment is more b-like or less (s+b)-like, respectively, than the observation; thus the confidence levels are defined over one-sided intervals. For $1-\mathrm{CL_b}$ ($\mathrm{CL_{s+b}}$) the integration starts from $-\infty$ ($+\infty$) and runs up to $Q_{observed}$.

When performing a search with small expected signal rates, it may happen that the observed number of candidates fluctuates significantly below the background expectation. In such cases

the mass limit might extend beyond the range of sensitivity of the search. In order to reduce the impact of such unintuitive but formally valid results from occuring, we take the ratio $\mathrm{CL_s}(m_\mathrm{H})$=$\mathrm{CL_{s+b}}(m_\mathrm{H})/\mathrm{CL_b}(m_\mathrm{H})$ as a conservative approximation to the confidence level for the signal-only hypothesis [22], and consider excluded at the 95% confidence level any hypothesis for which $\mathrm{CL_s}(m_\mathrm{H})$ is less than 0.05. The 95% confidence level lower limit for the Standard Model Higgs boson mass is then the highest test-mass m_H which yields $\mathrm{CL_s}(m_\mathrm{H})< 0.05$.

The quantity $1-\mathrm{CL_b}(m_\mathrm{H})$ measures the compatibility of the observation with the background hypothesis, and can thus be used as an indicator for the presence of a signal: a Standard Model Higgs boson with mass m_0 is expected to produce a drop in this quantity for $m_\mathrm{H}\approx m_0$. Background fluctuations may also produce such a drop. To minimize the risk of claiming a signal in the presence of background fluctuations, the threshold for the claim of discovery (evidence) is set at 5σ (3σ). Values of $1-\mathrm{CL_b} < 5.7\times10^{-7}$ ($1-\mathrm{CL_b} < 2.7\times10^{-3}$), with corresponding low probabilities of being background fluctuations, are interpreted as 5σ discovery (3σ evidence).

If the value of $Q_{observed}$ (and thus the integration bounds) is replaced by values obtained from Monte Carlo simulations of the real experiment, the expectations (median) for the confidence levels $1-\mathrm{CL_b}(m_\mathrm{H})$ and $\mathrm{CL_s}(m_\mathrm{H})$ are obtained. Of particular interest are the median expectation of $1-\mathrm{CL_b}(m_\mathrm{H})$ from simulated s+b experiments and the median expectation of $\mathrm{CL_s}(m_\mathrm{H})$ from simulated b experiments, since these indicate the potential of the available data set for discovery and exclusion, respectively, and the separation power of the data as a function of the test-mass.

The test-statistic adopted in the present LEP combination is the ratio of the likelihood function for the s+b hypothesis ($x=1$) to the likelihood function for the b hypothesis ($x=0$):

$$Q(m_\mathrm{H}) = \frac{\mathcal{L}(1)}{\mathcal{L}(0)}, \tag{3}$$

where the likelihood function is defined by

$$\mathcal{L}(x) = \prod_{k=1}^{N} \frac{exp[-(xs_k(m_\mathrm{H})+b_k)]\ (xs_k(m_\mathrm{H})+b_k)^{n_k}}{n_k!} \times \prod_{j=1}^{n_k} \frac{xs_k(m_\mathrm{H})S_k(m_\mathrm{H},i_{jk}) + b_kB_k(i_{jk})}{xs_k(m_\mathrm{H})+b_k}. \tag{4}$$

The index k runs over all independent contributions to the combined result: from different HZ final states and from data taken at different centre-of-mass energies and collected in different experiments. The symbol N stands for the number of such contributions ("channels"); n_k is the number of observed candidates in channel k and i_{jk} designates the position i of candidate j of channel k in the "space" of discriminating variables ($i\equiv[m_\mathrm{H}^{rec}, \mathcal{G}]$ in Section 3). The quantities $s_k(m_\mathrm{H})$ and b_k are the integrated signal and background rates in channel k with $s(m_\mathrm{H}) = \sum_{k=1}^{N} s_k(m_\mathrm{H})$ and $b=\sum_{k=1}^{N} b_k$ as the total expected signal and background in all channels. The functions $S_k(m_\mathrm{H},i)$ and $B_k(i)$ are the probability distributions of the discriminating variable(s) for the signal and background, respectively. The above notation assumes that the background-related quantities b and $B(i)$ do not depend on m_H. If the selection criteria in any one channel are explicitly m_H dependent, b and $B(i)$ have to be replaced by $b(m_\mathrm{H})$ and $B(m_\mathrm{H},i)$.

Appendix B:

Relation between Confidence Levels and Standard Deviations

To express the probabilities $1 - \mathrm{CL_b}$ and $\mathrm{CL_s}$ in terms of standard deviations (σ), we adopt a Gaussian approximation [23]. We express the significance of the observation using a convention for which $1 - \mathrm{CL_b} = 2.7 \times 10^{-3}$ (5.7×10^{-7}) would indicate a 3σ (5σ) deviation from the background expectation. The vertical scales indicated on the right-hand side in Figures 8 and 9 correspond to this convention.

Alternatively, one can use the convention reflected by the 68% and 95% probability bands in Figures 1, 2, 3, 10 and 11, which is convenient, for example, to discuss the statistical significance of a deviation, excess or deficit, with respect to the predicted background rate. Using this convention, $1 - \mathrm{CL_b} = 1.35 \times 10^{-3}$ (2.85×10^{-7}) would indicate a 3σ (5σ) excess while $\mathrm{CL_b} = 1.35 \times 10^{-3}$ (2.85×10^{-7}) would indicate a 3σ (5σ) deficit.

References

[1] P.W. Higgs, Phys. Lett. **12** (1964) 132; Phys. Rev. Lett. **13** (1964) 508; Phys. Rev. **145** (1966) 1156; F. Englert and R. Brout, Phys. Rev. Lett. **13** (1964) 321; G.S. Guralnik, C.R. Hagen, and T.W.B. Kibble, Phys. Rev. Lett. **13** (1964) 585.

[2] S. Weinberg, Phys. Rev. Lett. **19** (1967) 1264; *Elementary Particle Theory*, A. Salam, ed. N. Svartholm (Almquist and Wiksells, Stockholm, 1968),367.

[3] N. Cabibbo, L. Maiani, G. Parisi and R. Petronzio, Nucl. Phys. **B158** (1979) 295; R. Dashen and H. Neuberger, Phys. Rev. Lett. **50** (1983) 1897.

[4] M. Lindner, M. Sher and H.W. Zaglauer, Phys. Lett.**228B** (1989) 139; M. Sher, Phys. Lett. **317B** (1993) 159; *ibid.* **331B** (1994) 448; G. Altarelli and I. Isidori, Phys. Lett. **337B** (1994) 141; J.A. Casas, J.R. Espinosa and M. Quirós, Phys. Lett. **342B** (1995) 89.

[5] T. Hambye and K. Riesselmann, Phys. Rev. **D55** (1997) 7255.

[6] The LEP Electroweak Working Group, public page, http://lepewwg.web.cern.ch/LEPEWWG/ (updated July 2002).

[7] ALEPH, DELPHI, L3 and OPAL Collaborations, The LEP working group for Higgs boson searches, *Searches for Higgs bosons: Preliminary combined results using LEP data collected at energies up to 202 GeV*, CERN-EP/2000-055.

[8] ALEPH Collab., R. Barate et al., Phys.Lett. **B495** (2000) 1.

[9] L3 Collab., M. Acciarri et al., Phys. Lett. **B495** (2000) 18.

[10] OPAL Collab., G. Abbiendi et al., Phys. Lett. **B499** (2001) 38.

[11] DELPHI Collab., P. Abreu et al., Phys. Lett. **B499** (2001) 23.

[12] L3 Collab., M. Acciarri et al., Phys. Lett. **B517** (2001) 319.

[13] ALEPH, DELPHI, L3, OPAL, and the LHWG, *Search for the Standard Model Higgs Boson at LEP*, CERN-EP/2001-055.

[14] ALEPH Collab., R. Barate et al., Phys. Lett. **B526** (2002) 191.

[15] DELPHI Collab., *Final result on SM and MSSM neutral Higgs bosons*, DELPHI 2002-041-CONF-575.

[16] OPAL Collab., *" Search for the Standard Model Higgs Boson with the OPAL Detector at LEP"*, OPAL Physics Report PR367 (July 2002), to be submitted to Eur. Phys. Journal **C**.

[17] J. Ellis, M.K. Gaillard, and D.V. Nanopoulos, Nucl. Phys. **B106** (1976) 292;
J.D. Bjorken, Pproc. 1976 SLAC Summer Inst. Part. Phys., ed. M.C. Zipf (SLAC report 198,1977) 1;
B.W. Lee, C. Quigg and H.B. Thacker, Phys. Rev. **D16** (1977) 1519;
B.L. Joffe and V.A. Khoze, Sov. J. Part. Phys. **9** (1978) 50;
D.R.T. Jones and S.T. Petcov, Phys. Lett. **B84** (1979) 440;
F.A. Behrends and R. Kleiss, Nucl. Phys. **B260** (1985) 32.

[18] W. Kilian, M. Kramer, and P.M. Zerwas, Phys. Lett. **B373** (1996) 135.

[19] A.L. Read, Nucl. Instr. Methods **A 425** (1999) 357.

[20] K.S. Cranmer, Comput. Phys. Commun. **136** (2001) 198.

[21] ALEPH, DELPHI, L3, OPAL and the LEP Higgs Working Group, *Searches for Higgs bosons: Preliminary combined results from the four LEP experiments at* $\sqrt{s} \approx 189$ *GeV*; submitted to HEP-EPS'99, Tampere (Finland), July 1999.

[22] T. Junk, Nucl. Instr. Meth. Phys. Res. **A434** (1999) 435;
A. Read, in *1st Workshop on Confidence Limits*, CERN-2000-005.

[23] D.E. Groom et al., Eur. Phys. Journ. **C15** (2000) 1.

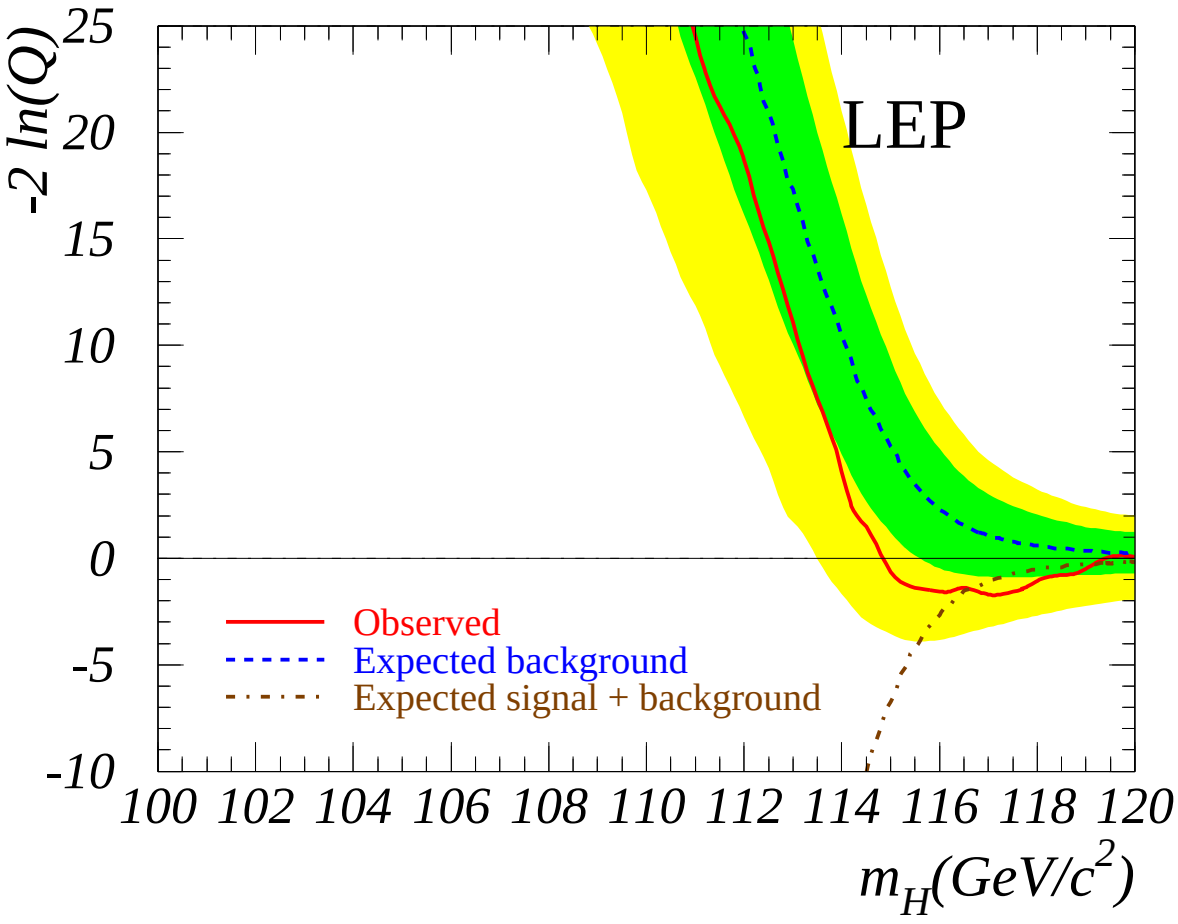


Figure 1: Observed and expected behaviour of the test-statistic $-2\ln Q$ as a function of the test-mass m_{H}, obtained by combining the data of all four experiments. The solid/red line represents the observation; the dashed/dash-dotted lines show the median background/signal+background expectations. The dark/green and light/yellow shaded bands represent the 68% and 95% probability bands (see Appendix B) about the median background expectation.

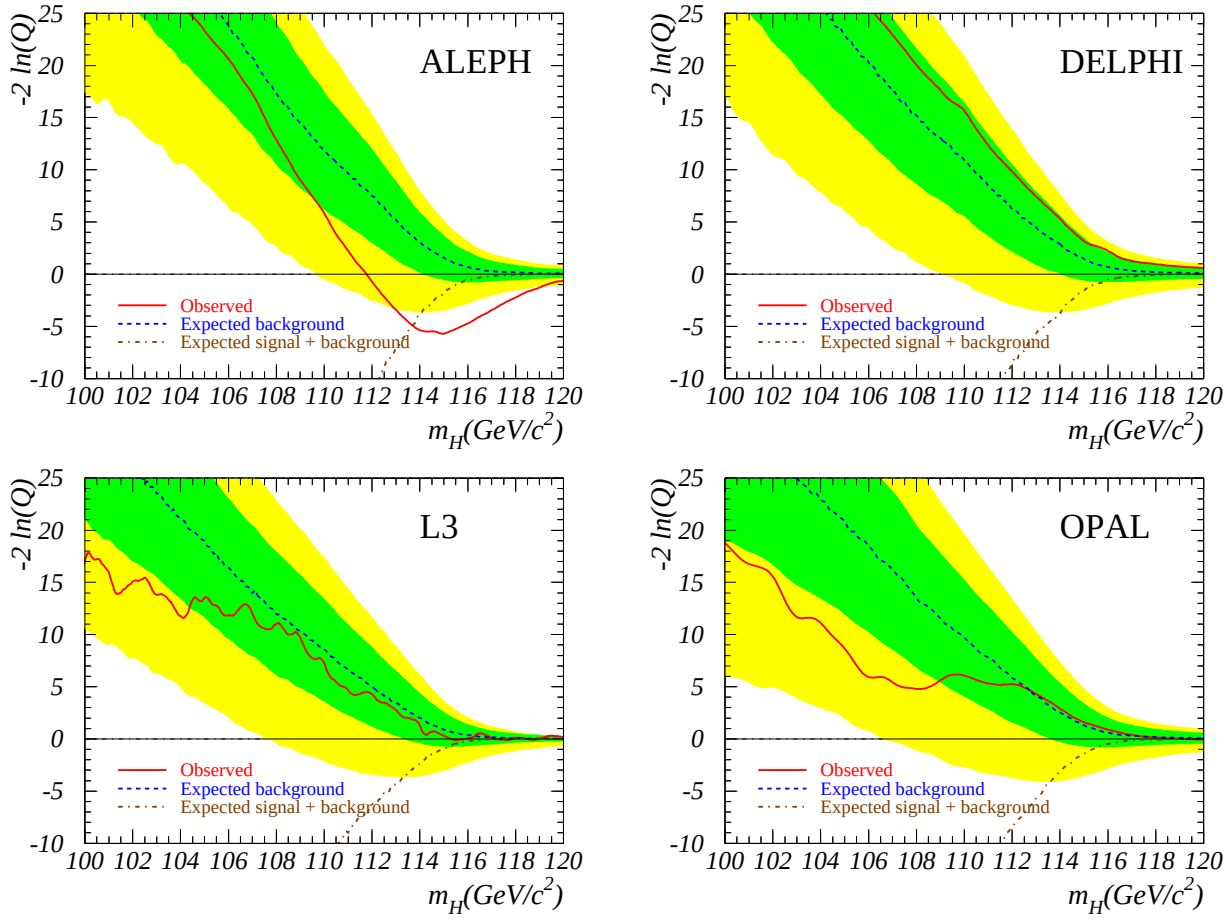


Figure 2: Observed and expected behaviour of the test-statistic $-2\ln Q$ as a function of the test-mass m_{H} obtained when the combination procedure is applied to the data sets of single experiments (see the caption of Figure 1 for the notations).

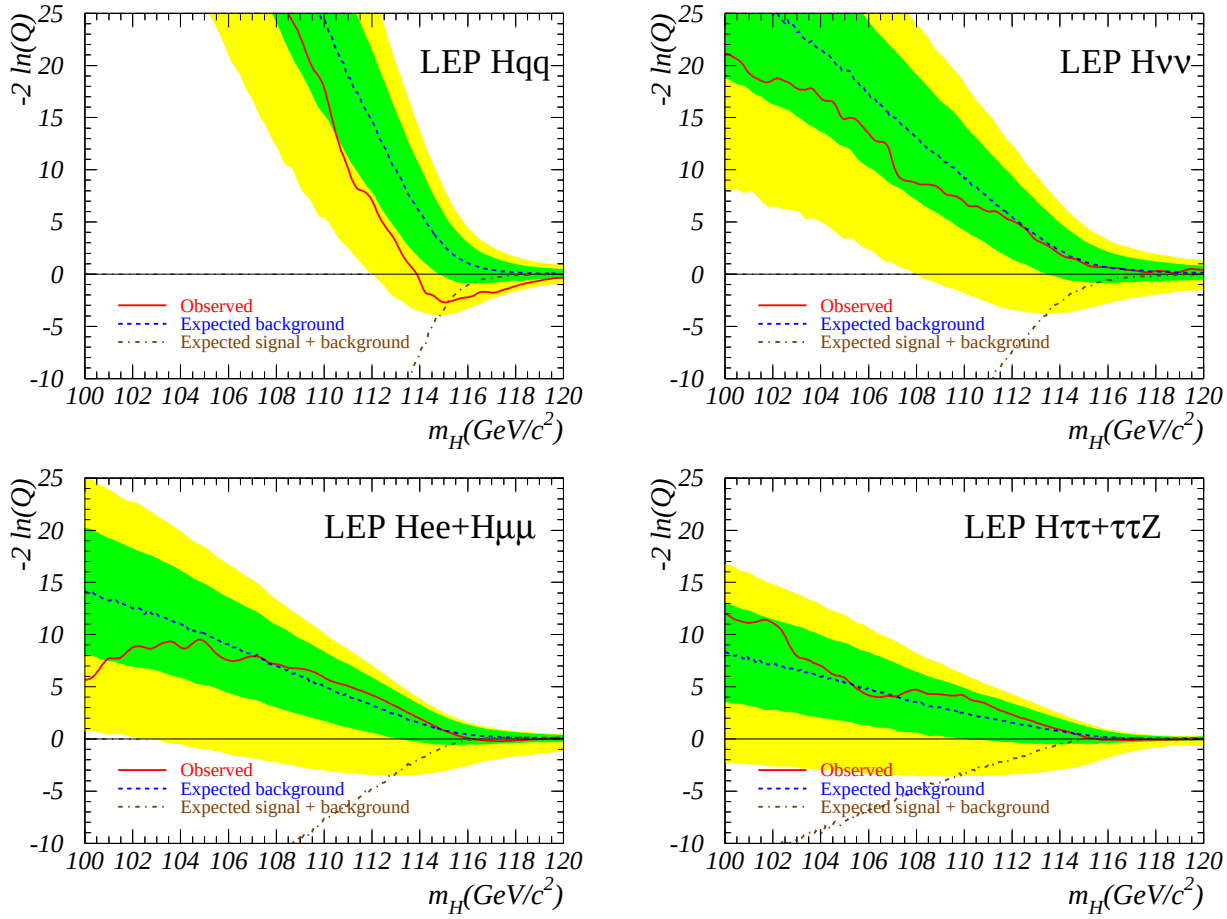


Figure 3: Observed and expected behaviour of the test-statistic $-2\ln Q$ as a function of the test-mass m_{H} obtained when the combination procedure is applied to the inputs corresponding to separated decay channels, all experiments combined (see the caption of Figure 1 for the notations).

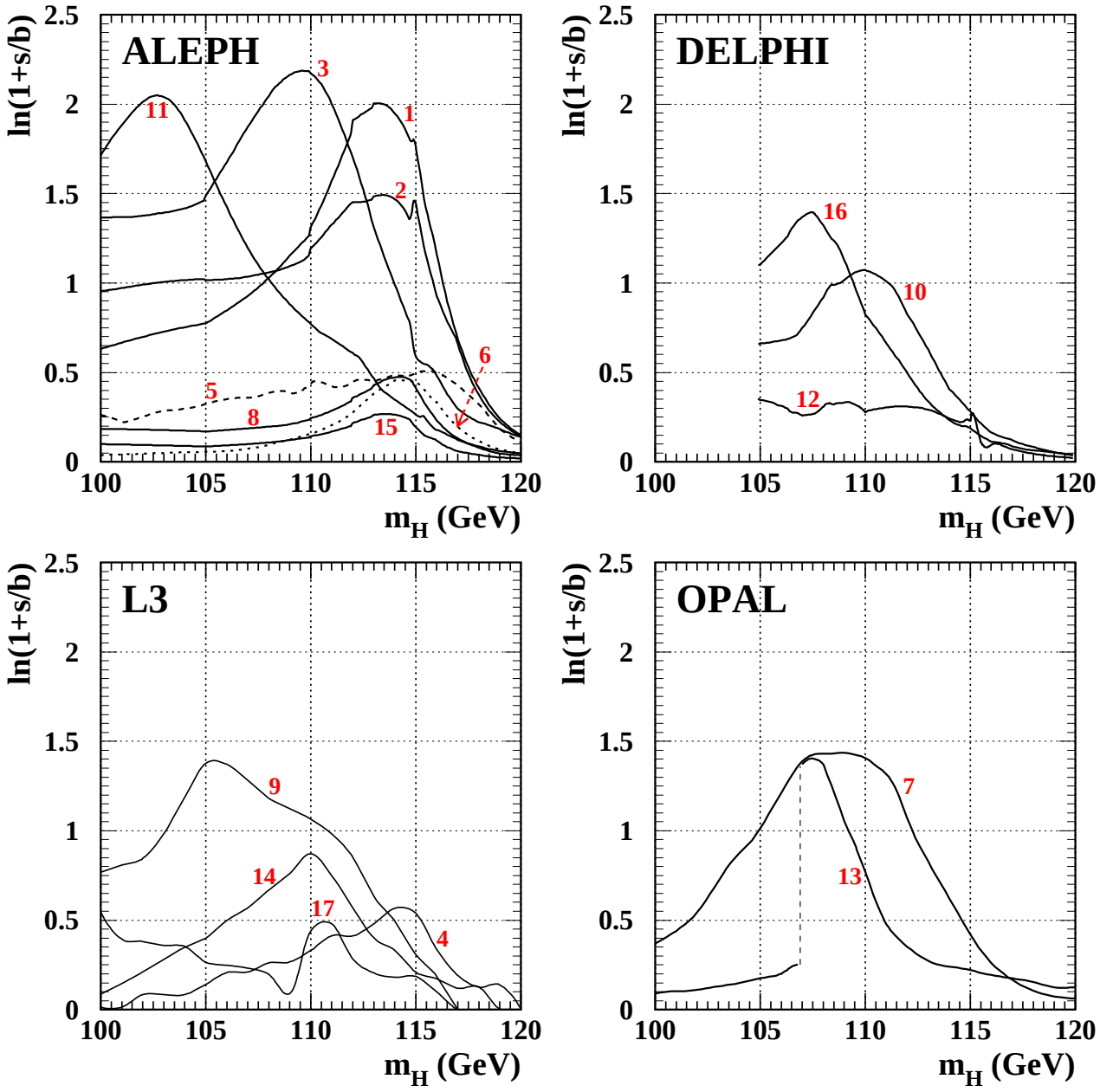


Figure 4: Evolution of the event weight $\ln(1+s/b)$ with test-mass $m_{\rm H}$ for the events with the largest contributions to $-2\ln Q$ at $m_{\rm H} = 115$ GeV. The labels correspond to the candidate numbers in the first column of Table 3. The sudden increase in the weight of the OPAL missing-energy candidate labeled "13" at $m_{\rm H} = 107$ GeV is due to the switching from the low-mass to high-mass optimization of the search at that mass. A similar increase is observed in the case of the L3 four-jet candidate labeled "17" which is due to a test-mass dependent attribution of the jet-pairs to the Z and Higgs bosons.

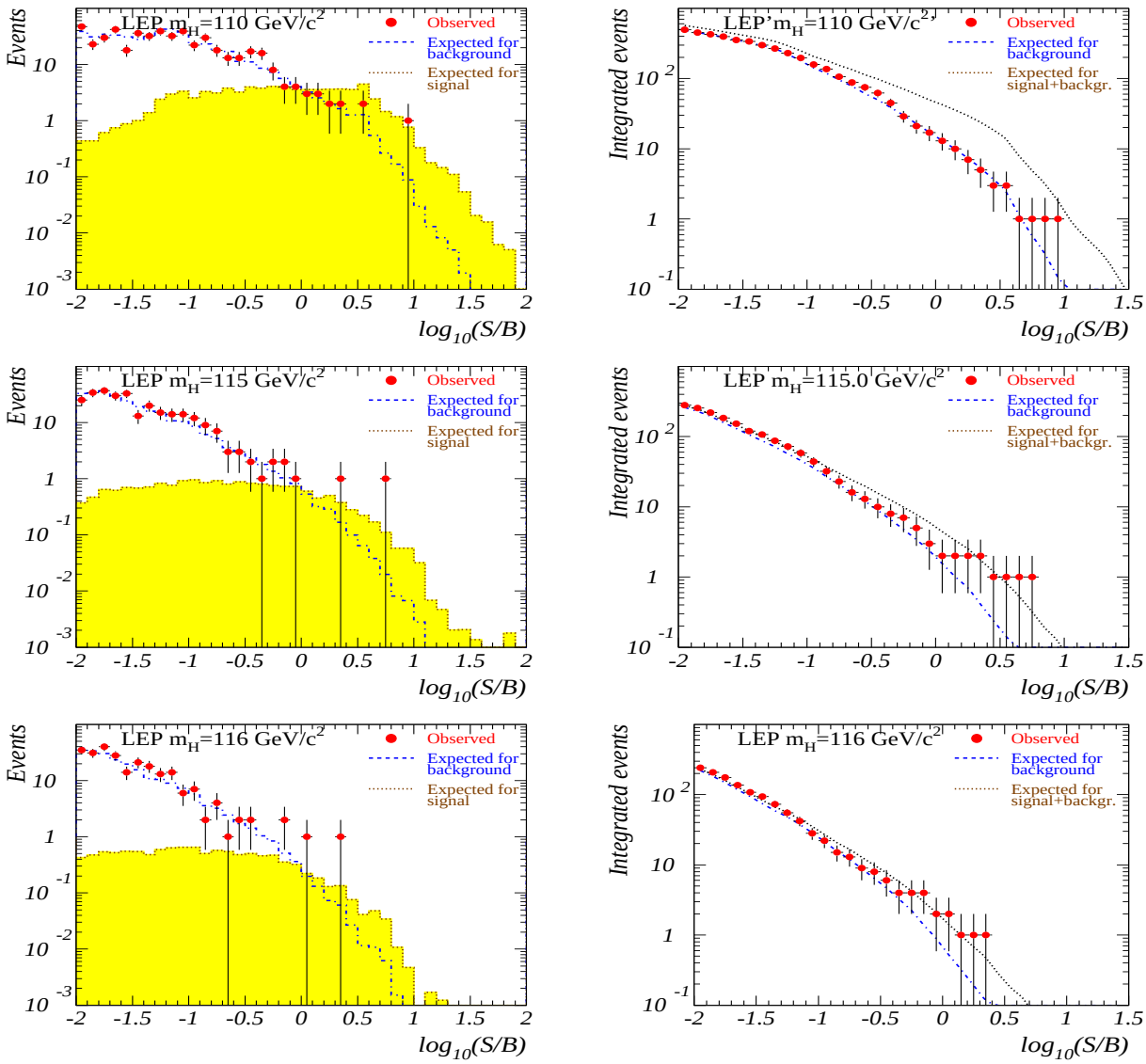


Figure 5: Left hand side: expected and observed distributions of $\log_{10} s/b$ for test-mass of $m_{\rm H}$ = 110, 115 and 116 GeV. White histograms: expected distributions for the background; shaded/yellow histograms: expected distributions for the signal; points with error bars: selected data. Right hand side: the integrals, from right to left, of the distributions on the left hand side. Dash-dotted and dotted lines: expectations for background and signal plus background, respectively.

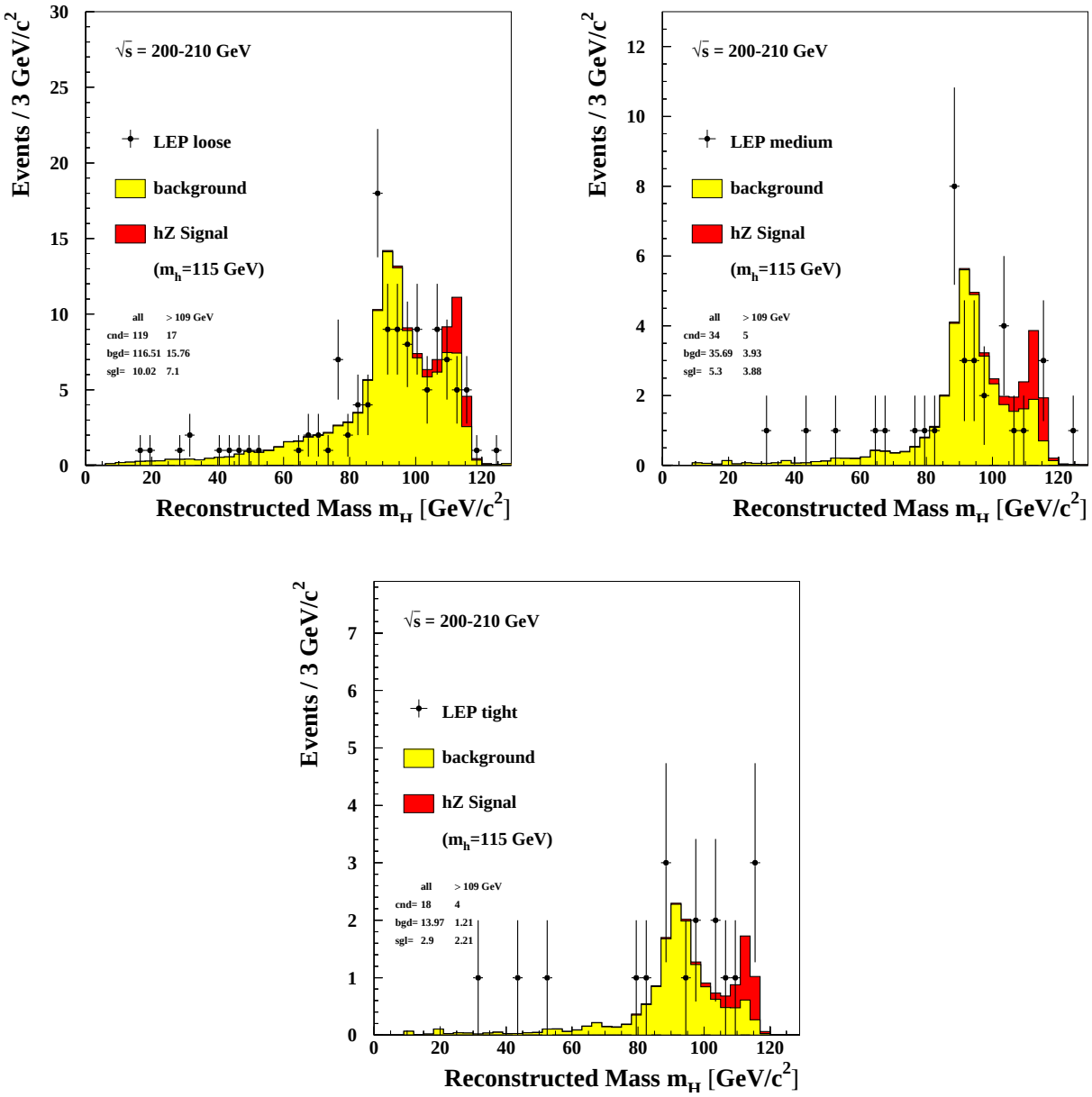


Figure 6: Distributions of the reconstructed Higgs mass, m_{H}^{rec}, obtained from three special, non-biasing, selections with increasing signal purity. In the loose/medium/tight selections the cuts are adjusted in such a way as to obtain, for a Higgs boson of 115 GeV mass, approximately 0.5/1/2 times as many expected signal as background events in the region $m_{\mathrm{H}}^{rec} > 109$ GeV.

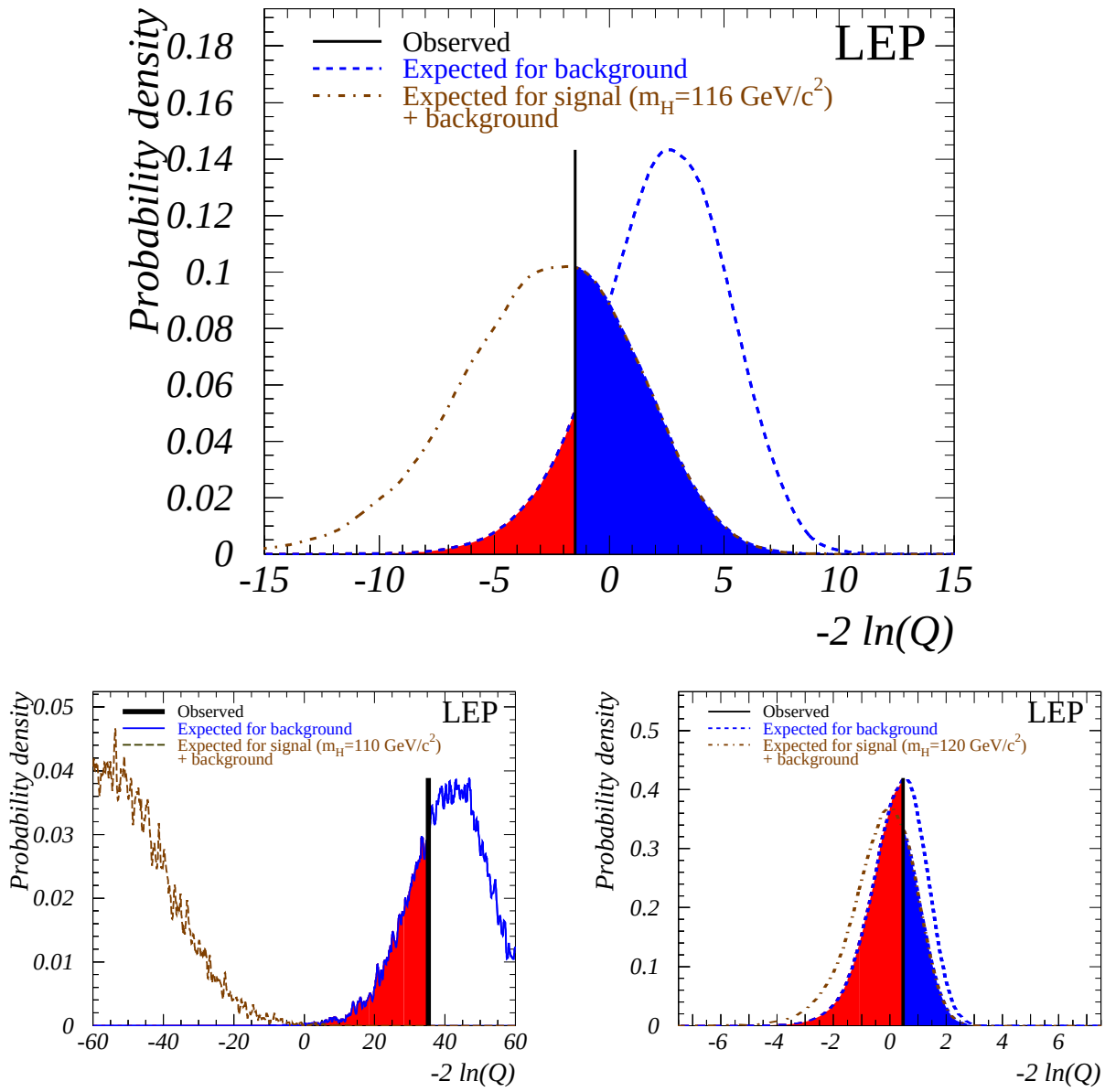


Figure 7: Probability density functions corresponding to fixed test-masses, for the background and signal+background hypotheses. The observed test-statistic $-2\ln Q$ is indicated by the vertical line. The light/red shaded areas, $1-\mathrm{CL_b}$, measure the compatibility with the background hypothesis and the dark/blue shaded areas, $\mathrm{CL_{s+b}}$, the compatibility with the signal+background hypothesis. Upper part: test-mass $m_\mathrm{H} = 116$ GeV; lower part: $m_\mathrm{H} = 110$ and 120 GeV.

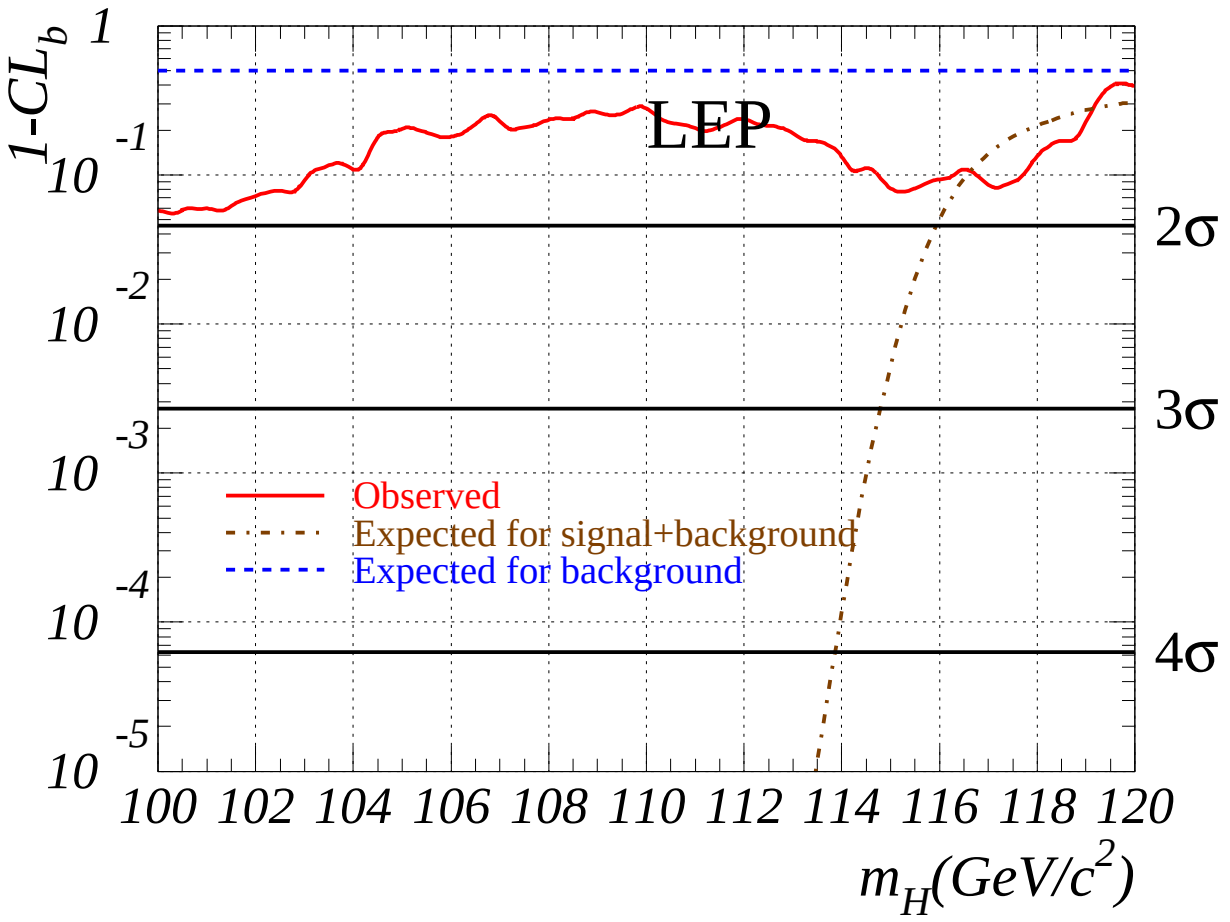


Figure 8: Probability $1 - \mathrm{CL_b}$ as a function of the test-mass m_H. Solid/red line: observation; dashed/dash-dotted lines: expected probability for the background/signal+background hypotheses. The horizontal solid lines indicate the levels for 2σ, 3σ and 4σ deviations from the background hypothesis (see Appendix B).

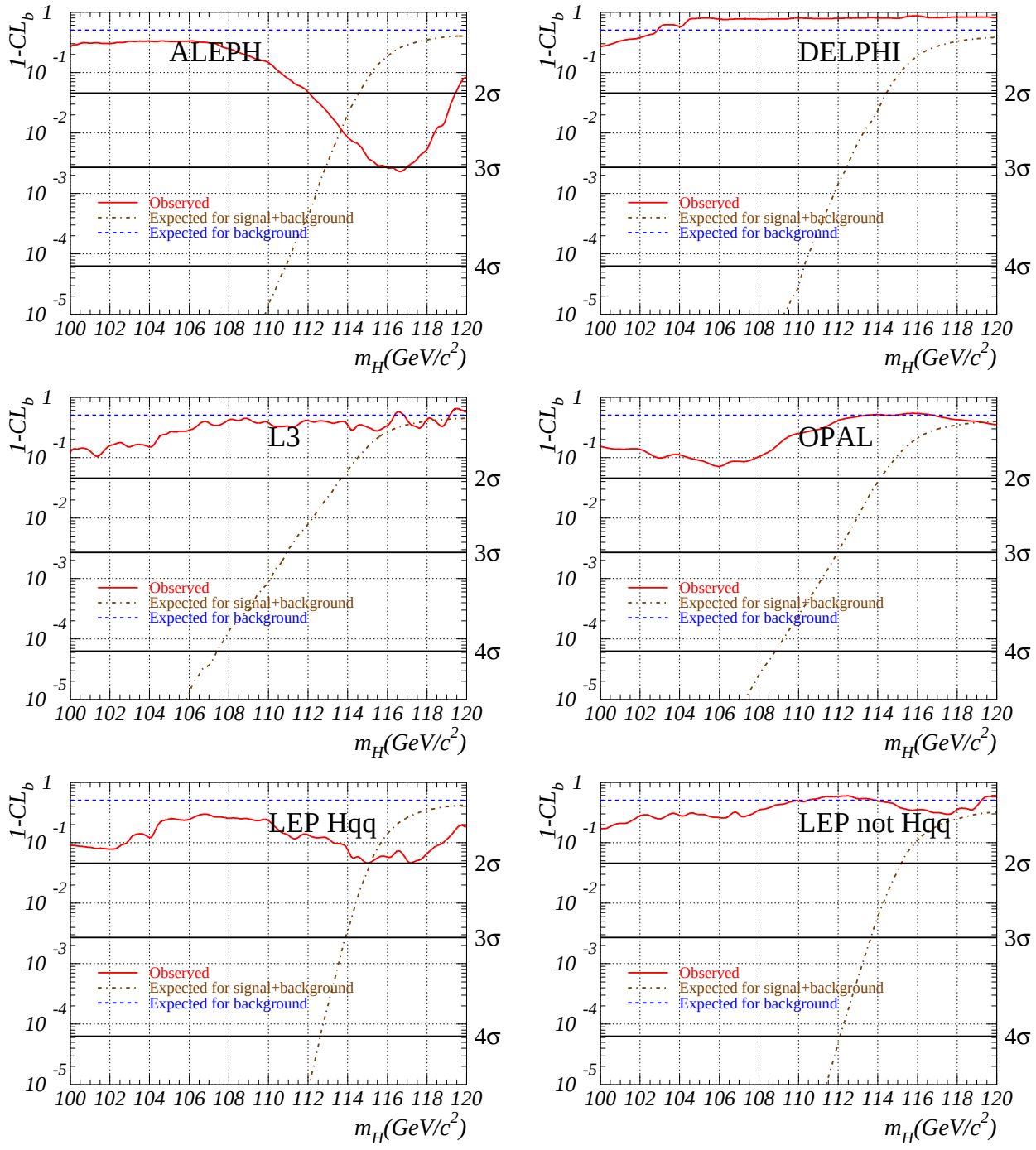


Figure 9: Probability $1 - \mathrm{CL_b}$ as a function of the test-mass m_H for subsets of the data. Upper four plots: individual experiments; lower two plots: the four-jet and all but the four-jet decay channel, with the data of the four experiments added. (See the caption of Figure 8 for the notations).

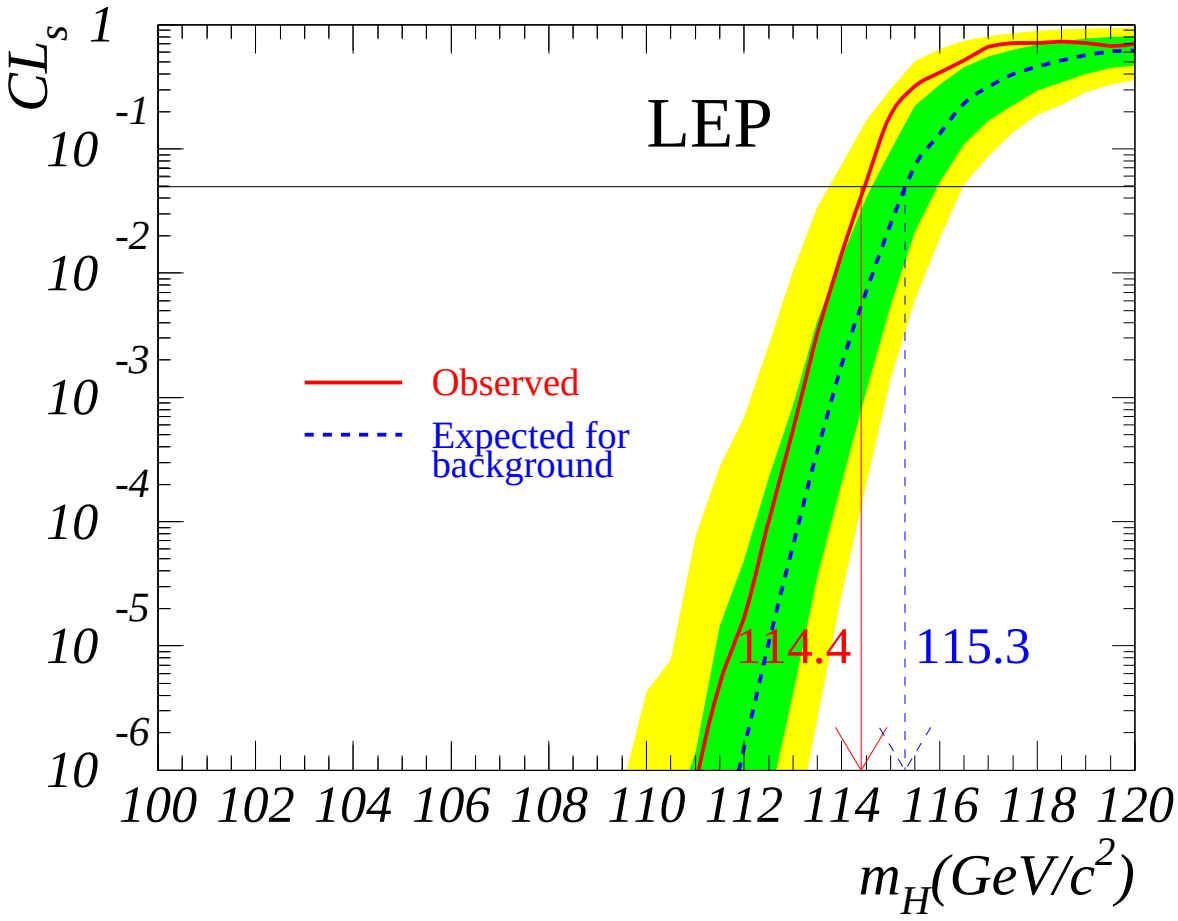


Figure 10: Confidence level CL_s for the signal+background hypothesis. Solid/red line: observation; dashed line: median background expectation. The dark/green and light/yellow shaded bands around the median expected line correspond to the 68% and 95% probability bands computed with a large number of simulated background experiments (see Appendix B). The intersection of the horizontal line at $CL_s = 0.05$ with the observed curve defines the 95% confidence level lower bound for the mass of the Standard Model Higgs boson (see Appendix A).

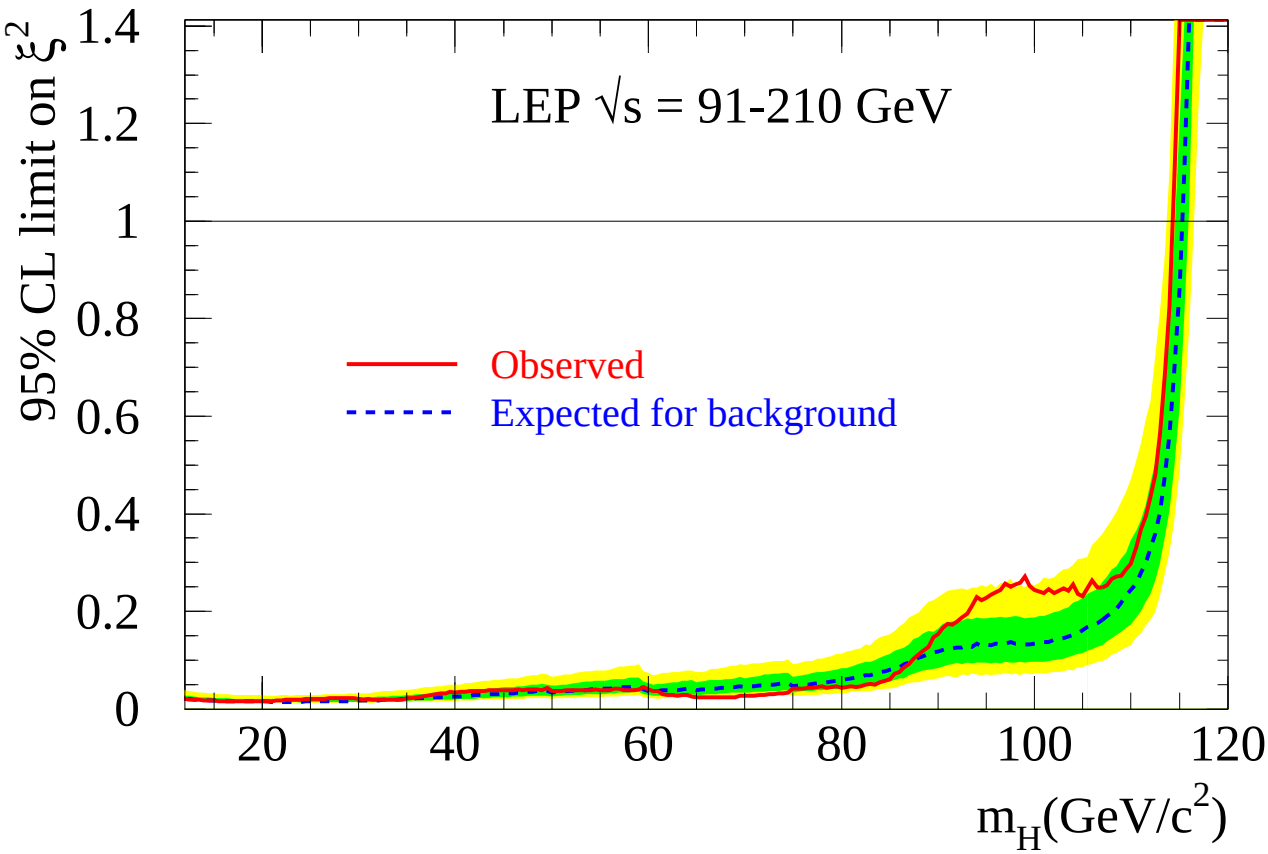


Figure 11: The 95% CL upper bound on ξ^2 as a function of the Higgs boson mass, where $\xi = g_{HZZ}/g^{SM}_{HZZ}$ is the HZZ coupling relative to the Standard Model coupling. The solid/red line represents the observed limit. The dark/green and light/yellow shaded bands around the median expected line correspond to the 68% and 95% probability bands (see Appendix B). The horizontal line corresponds to the Standard Model coupling. The structure in the vicinity of 100 GeV was reported in the LEP combination of 1999 [21] using data up to 189 GeV energy; its significance has not noticably increased with the addition of new data.